Accurate Noise Simulation of Microwave Amplifiers Using CAD

Ulrich L. Rohde
Compact Software
Paterson, NJ

Anthony M. Pavio
Texas Instruments
Dallas, TX

and

Robert A. Pucel
Raytheon Research Division
Lexington, MA

Introduction

The measurement of the noise parameters of microwave FETs and amplifiers is time-consuming and often inaccurate, especially at the higher frequencies, where the noise figure measurement error may be as high as 0.5 dB. This paper demonstrates the accuracy obtained with a CAD noise simulation program based on an improved noise model patterned after Fukui's approach. Starting from the noise model of the intrinsic FET and using nodal noise analysis, we show that CAD programs can provide accurate and reliable noise simulation of complex microwave circuits.

Noise Equations

It has been demonstrated many times that good noise performance can be obtained from microwave amplifiers and oscillators based on GaAs MESFETs. Using standard noise theory (as illustrated in Figure 1), a noise model for the GaAs FET has been derived by Pucel et al.[1] Applying certain approximations, Fukui[2,3] has derived simple equations for the four noise parameters based on this model:

$$F_{min} = 1 + K_1 f C_{gs} \sqrt{\frac{R_g + R_s}{g_m}}, \qquad (1)$$

$$R_n = \frac{0.8}{g_m}, \qquad (2)$$

$$R_{opt} = 2.2 \left(\frac{1}{4g_m} + R_g + R_s \right) \qquad (3)$$

and

$$X_{opt} = \frac{160}{fC_{gs}} \qquad (4)$$

where the coefficient $K_1 = 0.016$ and f is expressed in GHz. These (approximate) equations apply only to white noise generated in the FET, and they must be supplemented for low frequency applications by contributions representing the baseband (flicker) noise in order to explain the noise minimum with frequency illustrated in Figure 2. By including flicker noise and by modifying Fukui's equations based on a more accurate theoretical model, a new set of equations that better describes the intrinsic noise model shown in Figure 1 has been developed.

The flicker component of noise can be characterized by its "corner" frequency, which is designated f_c. This frequency is of special importance in the design of oscillators when AM-to-PM conversion is critical, because the amplitude noise spectrum of the flicker source modulates the carrier frequency of the oscillator and thereby is upconverted to the carrier band as phase noise. In linear amplifiers, this noise source must also be included when low frequency applications of FETs are considered. Therefore, ad hoc adjustments should be made to the equations for the four noise parameters, especially F_{min}. For instance, the expression for F_{min} is modified to

$$F_{min} \triangleq 1.0 + K_0 f C_{gs} \sqrt{\frac{R_g + R_s}{g_m}} + K_c \left(\frac{f_c}{f} \right) \qquad (5)$$

where the frequency f is expressed in Hz. The parameter f_c is typically in the order of 10 MHz for contemporary GaAs FETs, although some

[Continued on page 132]

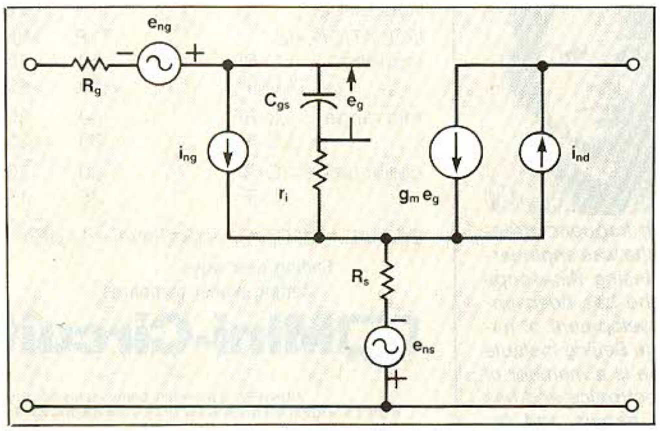

Fig. 1 FET noise model showing noise voltages and noise currents.

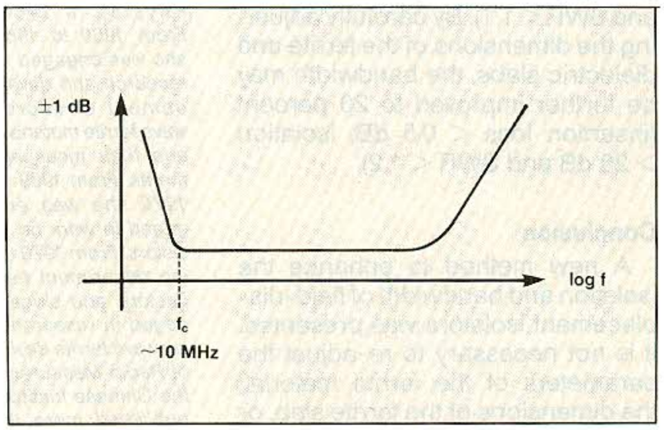

Fig. 2 Minimum noise figure of a GaAs FET as a function of frequency.

FETs have exhibited frequencies near 100 MHz. The constant K_c is a fitting factor.

The noise resistance, R_n, of the intrinsic FET is nearly frequency independent because it represents the white noise source accounting for the drain current fluctuations. However, in a packaged FET the noise resistance frequently exhibits a dip with frequency. This behavior can be attributed to package parasitic circuit elements interacting with the intrinsic device, specifically a resonance condition between the gate-source capacitance, C_{gs}, and the package inductances, L_s and L_g.

One may show that both the optimum source resistance and the optimum source reactance are proportional to the input reactance of the gate-source capacitance, a result that differs with Fukui's Equation 3 above, which postulates a frequency-independent optimum source resistance.

The four noise parameters listed above usually are incorporated in a CAD program as elements of the noise correlation matrix.[4] The derivation of the noise matrix, though straightforward, can be rather lengthy, especially when parasitic elements of the complete equivalent circuit of the FET shown in Figure 3 are included. However, once derived, the noise matrix can be treated in a fashion similar to the Y and Z matrix of the transistor when calculating the noise performance of an amplifier. These computations are resident in the Super-Compact software. The derivation for the noise correlation matrix as shown in the Appendix on page 141 was presented by Prof. Russer at the Users' Group meeting of Compact Software at the MTT-S Symposium in May 1988.

Modeling of the Circuit

The new noise model was applied to a variety of monolithic integrated circuits (MMICs). MMICs utilize mostly distributed elements. Figure 4 illustrates a layout of the metalization interconnect pattern of a single-stage MMIC amplifier. Figure 5 shows the layout in detail. The most accurate circuit description used in a CAD program would reflect the details of this layout—such as the bends and junctions. For modeling purposes, the designer often approximates the actual distributed layout with a combination of distributed and lumped elements.

Active elements such as FETs are usually represented by their equivalent circuit models. By introduction of a physical scaling factor for the transistor, the various equivalent circuit parameters can be scaled to different peripheries and optimized for the application at hand. Figure 6 illustrates a Super-Compact circuit file that incorporates this type of scaling. The FET models from foundries such as TriQuint allow

[Continued on page 134]

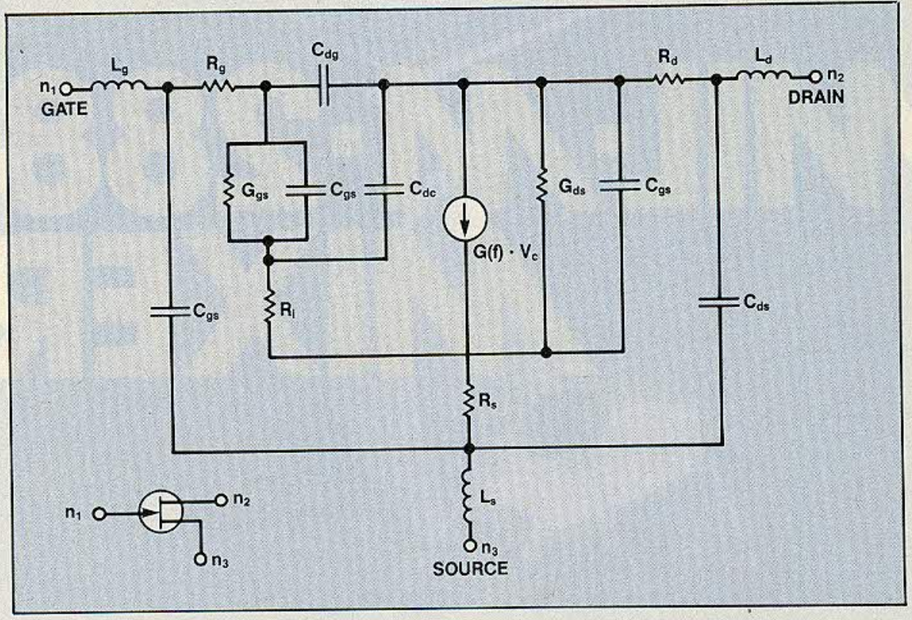

Fig. 3 Equivalent circuit of a linear FET including parasitic elements.

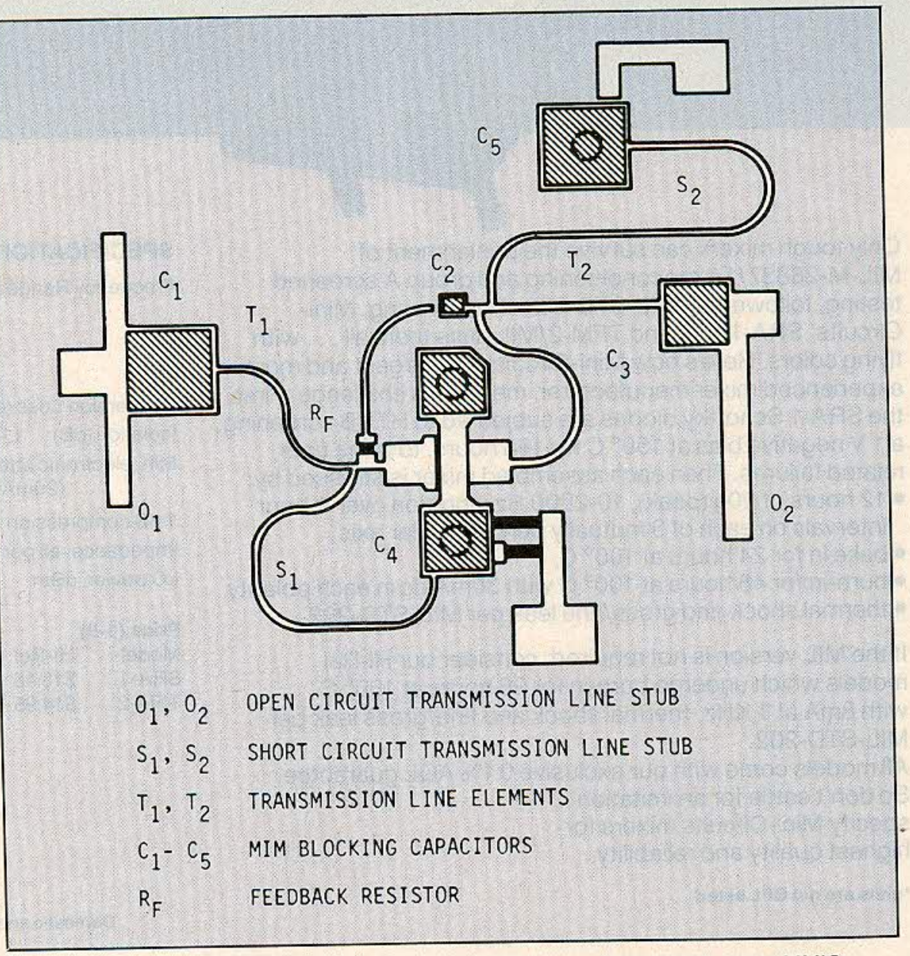

Fig. 4 Layout of the metalization interconnected pattern of a single-stage MMIC.

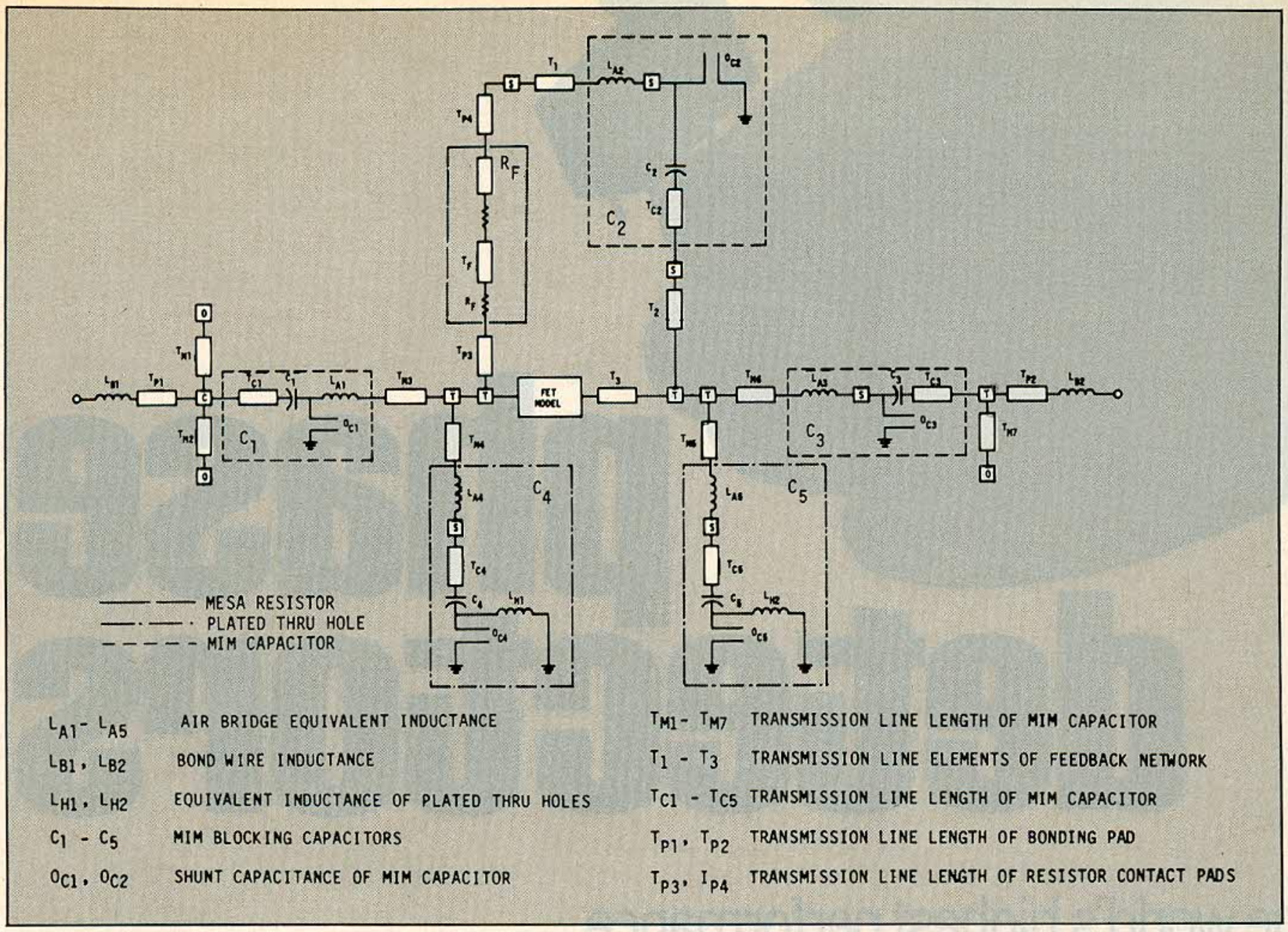

Fig. 5 Layout of the same amplifier as in Figure 4, but in this case all the MMIC components are broken down into final details for modeling purposes.

```
SUPER COMPACT PC  10/02/88  09:58:44  File: fetnoise

 **************************************************
 * TEXAS INSTRUMENTS INTERDIGITAL FET MODEL        *
 * LENGTH NORMALIZED TO 300 MICRONS                *
 **************************************************
z:.63
 BLK
   FET 1 2 0 G=(.045*Z) CGS=(.3PF*Z) T=3E-12 CDG=(.02PF*Z)
 +  CDS=(.085PF*Z) RG=(4/Z) RI=(4/Z) RS=(3.5/Z) RD=(3.8/Z) LS=.02NH
 +  GDS=(.0029*Z) nfac=.5
 *
 * EXAMPLE FOR NOISE  MODELING  'ALT N FOR NOISE ON' FOR PC
 * TYPE 'NOISE ON' FOR MAIN FRAME
 * SET UP TABLE FOR NOISE PARAMETERS
 * available from scompact pc ver. 4.0 and mainframe 1.95
 * fet drain pad
   TRL 2 3 W=2.9MIL P=.8MIL SUB1
 TIFET: 2POR 1 3
 END
 *
 FREQ
 STEP .1GHZ 20GHZ .2GHZ
 * 19.8GHZ
 * STEP 1GHZ 20GHZ .5GHZ
 END
 *
 *
 OUT
   PRI tifet s
 END
 *
data
sub1:ms h=6mil er=12.9 met1=au 5um tand=0.0004
end
```

Fig. 6 Printout of a Super-Compact listing showing the equivalent circuit values for the Texas Instruments 300 μm device and the scaling factors.

one to express the equivalent circuit elements in terms of other device design parameters, such as the number of gate fingers, pinchoff voltage, bias voltages and the like. Thus, by varying these design parameters, one has added flexibility to optimize the equivalent circuit elements. Figure 7 presents a circuit file in Super-Compact 4.0 based on TriQuint foundry data.

Verification of Modeling

Our modified noise model and the CAD software based on it were validated by applying them to three MMICs.

The first circuit was a two-stage feedback amplifier designed and fabricated by Texas Instruments.[5] Figure 8 is the corresponding Super-Compact circuit file. The individual distributed elements were described by models resident in the Super-Compact software. Because it was not possible to model any

[Continued on page 136]

```
SUPER COMPACT PC  10/03/88  16:42:45  File: fb300b

* FB_300.ckt june 18/88
* 2 stage amplifier 2...6 GHz
* 300 um FET vds=4.0 Id=Idss/2
* using 2 constant current sources
blk
ind 1 2 l=.3nh
cap 2 0 c=.045Pf
bwire:2por 1 2
end
**************************************************
* Main circuit
**************************************************
blk
bwire  1  2
fiND   2  3        TYPE=1  L=1.e-9  H=7MIL  TQ
FFET   3  4  5     TYPE=1  W=50UM  N=6  XIDS=0.5  VDS=4.0 TQ
cap    4  5        c=0.07pf
FRES  3  7         TYPE=1  R=140  W=10UM  H=7MIL    TQ
FIND   4  6        TYPE=1   L=1.800E-9  H=7MIL   TQ
FCAP   6  7        TYPE=1  C=10000FF  TQ
Fres    7  15      TYPE=2  R=1000   W=10UM   H=7MIL   TQ
FFET   6  14  6    TYPE=1  W=50UM  N=3  XIDS=1  VDS=4.0 TQ
FCAP    14 15      TYPE=1  C=10000FF  TQ
bwire  15 0
ind    5  50     l=.05nh    Q=8   F=10GHZ
bwire  50 0
bwire  50 0
bwire  50 0
ind     7  8      l=0.3nh   Q=8  F=10GHZ
FFET    8  9  10    TYPE=1  W=50UM  N=6  XIDS=0.5  VDS=4.   TQ
FFET    8  9  10    TYPE=1  W=50UM  N=6  XIDS=0.5  VDS=4.   TQ
cap     9  10     c=.05pf
FRES    8  12     TYPE=1   R=450  W=10UM  H=7MIL    TQ
fIND    9  11     TYPE=1  L=1600E-12  H=7MIL  TQ
Fcap     11 12    TYPE=1  c=10000FF   TQ
FFET    11 14 11    TYPE=1 W=50UM N=3 XIDS=1 VDS=4 TQ
ind     10 50     l=.05nh
bwire   50 0
bwire   50 0
bwire   50 0
bwire   12 13
amp:2por 1 13
end
**************************************************
 * TriQuint INTERDIGITAL FET MODEL 1um GATE        *
 * LENGTH NORMALIZED TO 300 MICRONS  IDS = 15 %   *
**************************************************
 *
 FREQ
   STEP 1ghz 8GHZ .5GHZ
 END
 *
 *
 OUT
  PRI amp s
 END
```

Fig. 7 Super-Compact circuit file listing of a 2 to 6 GHz amplifier using TriQuint foundry elements. This circuit can be utilized for noise because the foundry FET generates all the frequency-dependent noise data.

```
* INPUT MATCHING NETWORK
*
*
BLK
*
*** INPUT PAD
 IND    1    2   L=.15NH
 TRL    2   90   W=9.5MIL   P=2.0MIL  GAS4
 OPEN 90    0    W=9.5MIL             GAS4
 TRL    2    3   W=9.5MIL   P=2.5MIL  GAS4
*
*** OPEN STUB
 TEE    4    5    3   W1=7.5MIL  W2=7.5MIL  W3=9.5MIL  GAS4
 TRL    4   70   W=7.5MIL  P=3.92MIL  GAS4
 BEND  70 72    W=7.5MIL  GAS4
 TRL   72   7    W=7.5MIL  P=7.08MIL   GAS4
 OPEN   7        W=7.5MIL  GAS4
*
*** SERIES CAP
 TRL    5    9   W=7.5MIL  P=3.75MIL  GAS4
 CAP    9   10   C=8PF
 TRL  10   11    W=7.5MIL  P=3.75MIL  GAS4
 STEP 11   12    W1-7.5MIL  W2=.5MIL  GAS4
 IND  12   13    L=.001NH
*
***SERIES TRANSMISSION LINE
 TRL  13   14   W=.5MIL  P=15MIL  GAS4
*
*
IMN:  2POR  1  14
END
*
```

(a)

```
**************************************************
*
*                    FEEDBACK NETWORK
*
BLK
*
***TRANS. LINES TO JUNCTION
*
STEP  1  61  W1=.5MIL  W2=1.6MIL  GAS4
TRL  61  51  W=1.6MIL   P=1MIL     GAS4
STEP  4  64  W1=.5MIL  W2=1.6MIL  GAS4
TRL  64  54  W=1.6MIL   P=1MIL     GAS4
*
***INPUT JUNCTION
 CROS  51   2   3   54   W1=1.6MIL  W2=1.6MIL  W3=1.6MIL  W4=1.6MIL
+ GAS4
 TRL    3  30   W=1.6MIL  P=1MIL  GAS4
 STEP  30  5   W1=1.6MIL   W2=4.2MIL  GAS4
*
***FET MODEL
 FETMOD  5  6  7
*
***FET SOURCE NETWORK
 IND    7    9   L=LAB
 IND    9    0   L=LVIA
 IND    7    8   L=LAB
 IND    8    0   L=LVIA
*
***GATE SHUNT INDUCTOR
 GSI1    4  200
 IND   200  0  L=LVIA
*
***FEEDBACK LOOP
 FBLP1  2  17
*
***DRAIN INDUCTOR
 STEP  6  10    W1=2.9MIL W2=0.5MIL  GAS4
 TRL  10  11     W=.5MIL   P=21MIL    GAS4
*
***OUTPUT NETWORK
 STEP  11  12     W1=.5MIL  W2=1.6MIL    GAS4
 TRL   12  13     W=1.6MIL  P=1.0MIL    GAS4
 STEP  13  14     W1=1.6MIL  W2=3.5MIL  GAS4
 TRL   14  15     W=3.5MIL  P=.9MIL     GAS4
 TEE   17  15  16  W1=3.5MIL  W2=3.5MIL  W3=1.6MIL  GAS4
*
FBFET1:  2POR  1  16
END
*
```

(b)

Fig. 8 Super-Compact circuit file for the two-stage feedback amplifier: (a) input matching network; and (b) feedback network.

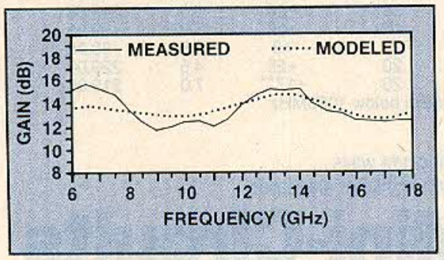

Fig. 9 Comparison between measured and predicted gain of the amplifier shown in Figure 11.

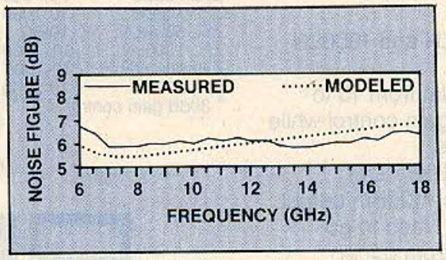

Fig. 10 Noise performance of the two-stage amplifier showing measured vs modeled results.

parasitic coupling between the various elements in the circuit, and because the FET elements could only be assigned nominal values (since they could not be characterized individually), some discrepancies were expected between the predicted and measured gain and noise performance. Figure 9 is a comparison of the predicted and measured gain.

[Continued on page 139]

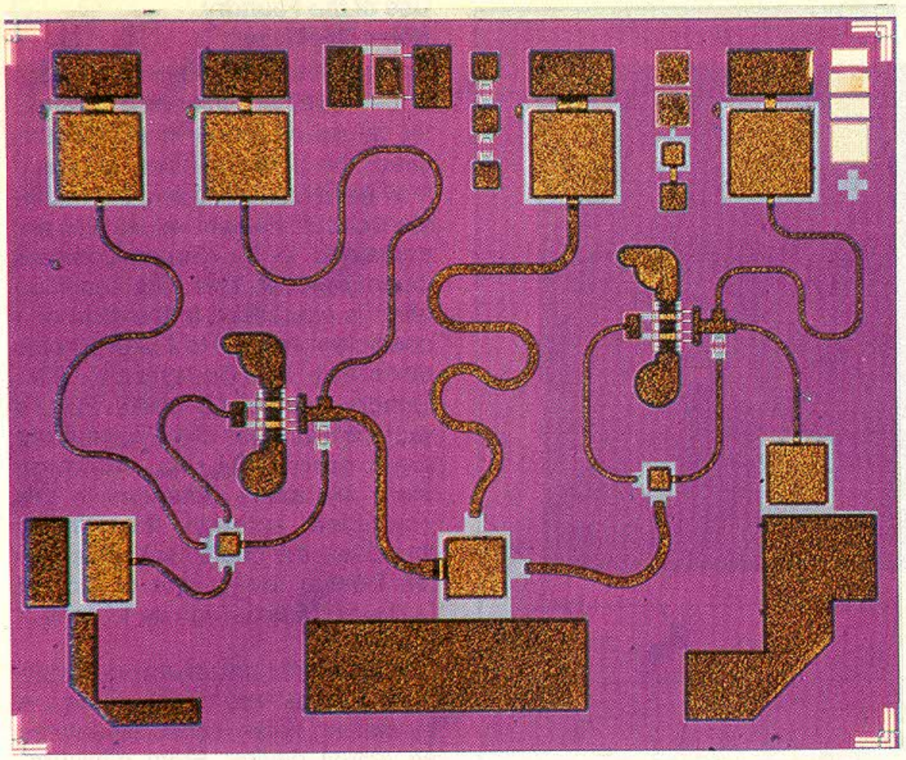

Fig. 11 Circuit layout of a two-stage feedback amplifier designed and fabricated by Texas Instruments.

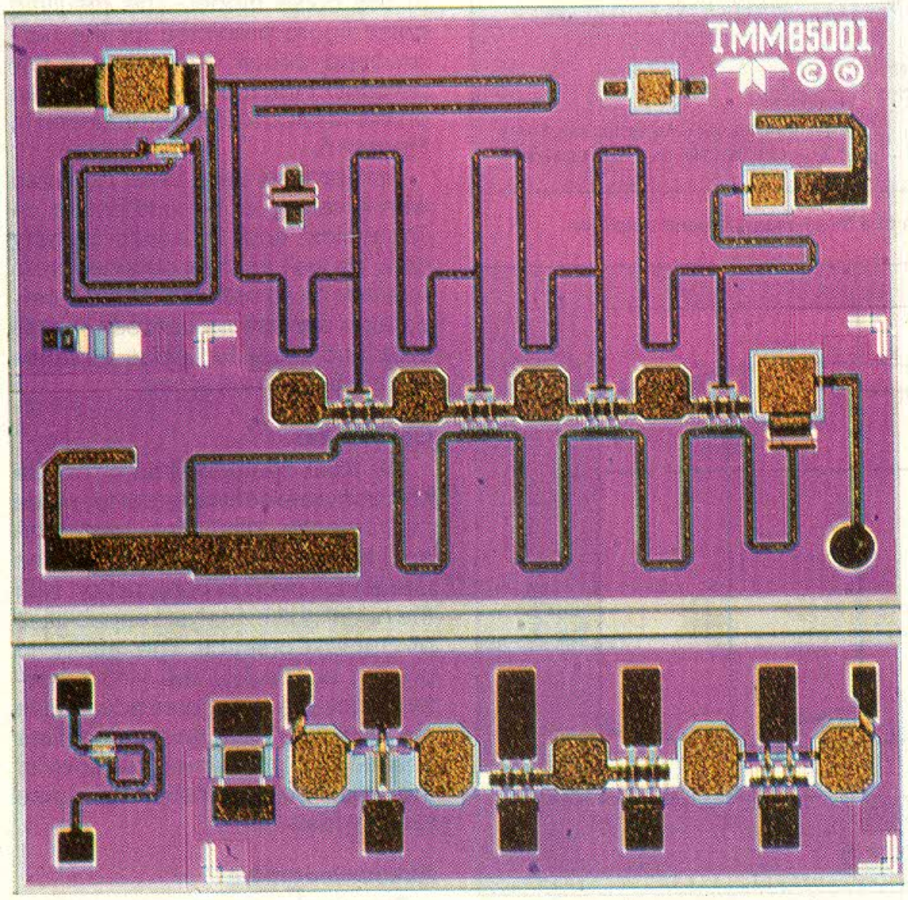

Fig. 12 Photograph of the distributed amplifier operating from 2 to 18 GHz, with a noise figure from 5 to 17 dB and 6 to 70 dB of gain.

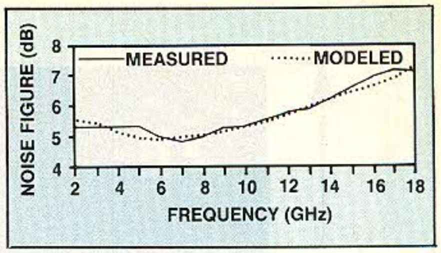

Fig. 13 Measured vs predicted performance of the distributed amplifier.

Since the gain response is not predicted accurately, one can only expect fair agreement between the predicted and measured noise performance. Furthermore, some errors will be introduced by the noise measurement (for example, by the noise analyzer itself) and by the impedance mismatch between the circuit and the noise source. Figure 10 shows how the predicted and measured noise performance compare. If we assign a total accumulated uncertainty in the measured noise figure of as much as 0.6 dB, which is a reasonable assumption for such high noise figures, the agreement between the measured and modeled noise performance can be considered satisfactory. Figure 11 is a photograph of the two-stage amplifier circuit layout.

The second circuit analyzed, shown in Figure 12, was a distributed amplifier designed by Teledyne and fabricated by Texas Instruments.[6] The layout of this circuit was somewhat easier to describe with accuracy in a circuit file based on existing CAD models. As a consequence, closer agreement between the measured and predicted circuit performance was obtained, as shown in Figure 13.

Both broadband amplifiers described above exhibited high noise figures compared to what one should expect from narrowband designs based on the same FETs. Therefore, a narrowband example should provide a more critical test of the accuracy of the noise model. Figure 14 illustrates a three-stage X-band amplifier operating in the 8 to 12 GHz frequency band. This device exhibited in production a noise figure of 2 dB with a 0.2 dB tolerance band. This amplifier was modeled using Super-Compact PC Version 4.0. Good agreement was obtained with the measured gain and with the measured noise performance.

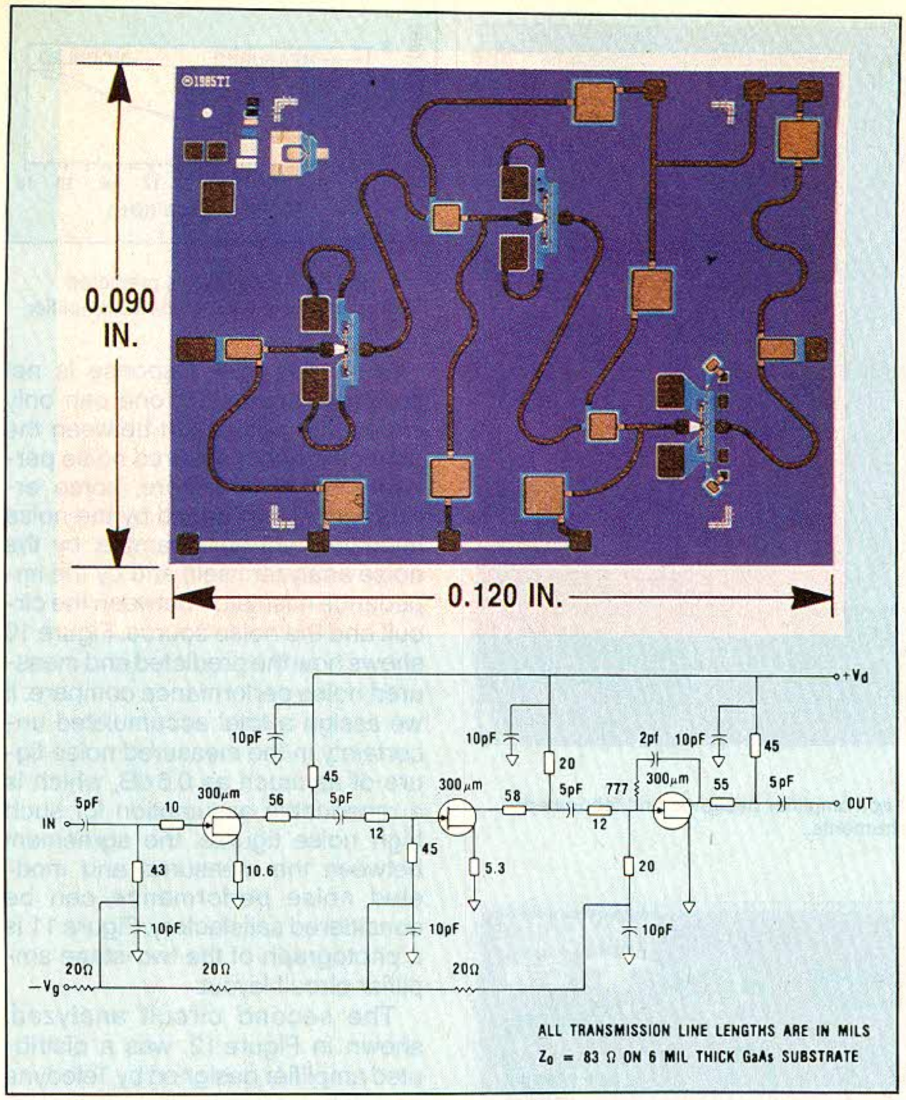

Fig. 14 Layout and schematic diagram of a three-stage X-band amplifier.

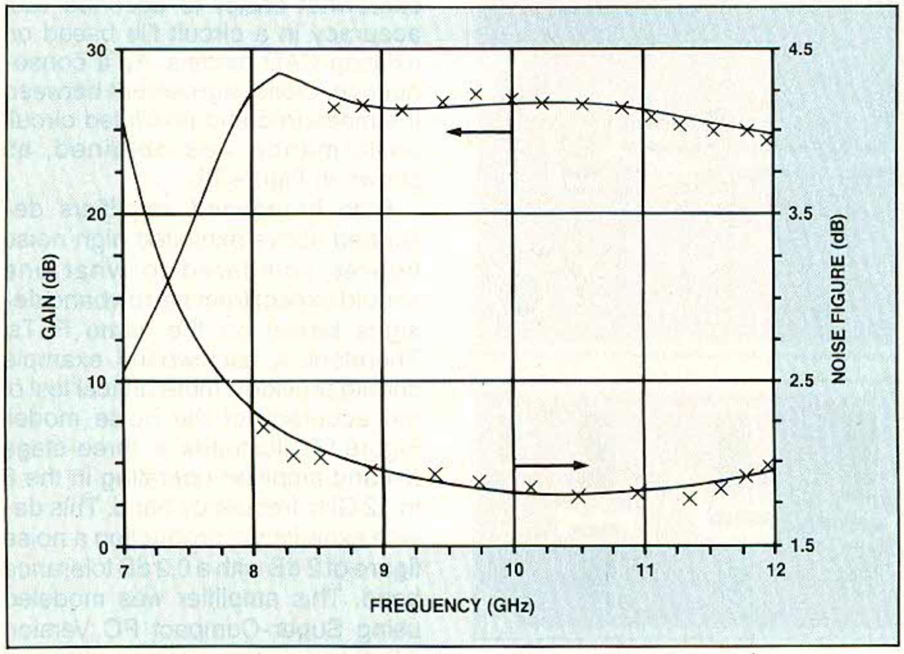

Fig. 15 Gain and noise plot prediction of the TI X-band model EG8021 using Super-Compact PC 4.0. The X marks on the plot indicate measurements done by Texas Instruments.

Use of the Foundry Noise Coefficient

When foundry models are used in Super-Compact, the noise parameter values no longer must be supplied; the bias condition at which they were measured and the equivalent circuit element values also are contained in the Super-Compact foundry model. This bias condition often is expressed in the form of a coefficient related to Fukui's noise constant, K_1 (Equation 1). The foundry coefficient, unlike Fukui's value, is a function of the normalized drain current, I_{ds}/I_{dss}. Although there are some variances in this coefficient amongst the various foundries, the coefficient value varies from a lower limit of 0.5 for I_{ds}/I_{dss}=0.15 to as high as 1.7 for I_{ds}/I_{dss}=0.5.

If this coefficient value is not available, the best way to determine it is by making noise measurements on an actual device. From measurements taken at 10 GHz at a drain current corresponding to 15 percent I_{dss}, a noise coefficient of 0.5 was obtained. This value was used in the noise model. The resulting noise figure predicted for the narrowband circuit was within a few percent of the measurements taken on the MMIC. This is summarized in Figure 15.

Similar tests have been repeated with a variety of circuits based on Tachonics' and TriQuint's foundry data, as well as data obtained from Avantek. In all of these cases, comparable agreement between measured and predicted noise performance has been obtained.

Conclusion

We have demonstrated a reliable and accurate software tool for noise performance simulation based on an improved noise model for the GaAs FET used in conjunction with the nodal noise analysis capabilities of Super-Compact. The ability to predict accurately the noise performance is a significant advance in the design of low noise amplifiers destined for production because of the possible elimination of noise testing costs.[7,8,9]

Acknowledgment

This study represents a cooperative effort between Raytheon Co., Texas Instruments Inc. and Compact Software.

Appendix: Analysis of Linear Noisy Networks using Correlation Matrices

The autocorrelation and cross-correlation spectra $C_{ij}(f)$ of the noise sources of a linear network are given by

$$C_{ij}(f) = \lim_{T\to\infty} \frac{1}{2T} \langle \underline{S}_{iT}(f)\, \underline{S}^{*}_{jT}(f) \rangle, \qquad (1)$$

where $\underline{S}_{iT}(f)$ and $\underline{S}_{jT}(f)$ are the spectra of the signals windowed in the time domain. The correlation spectra of the equivalent noise sources of a network or of an n-port are represented by the correlation matrix:

$$C(f) = \begin{bmatrix} \underline{C}_{11}(f) & \underline{C}_{12}(f) \ldots & \underline{C}_{1n}(f) \\ \underline{C}_{21}(f) & \underline{C}_{22}(f) \ldots & \underline{C}_{2n}(f) \\ \vdots & \vdots & \\ \underline{C}_{n1}(f) & \underline{C}_{n2}(f) \ldots & \underline{C}_{nn}(f) \end{bmatrix} \qquad (2)$$

The correlation matrix, C(f), can be written as the ensemble average of the product of the vector

$$S_T(f) = \begin{bmatrix} \underline{S}_{1T}(f) \\ \vdots \\ \underline{S}_{nT}(f) \end{bmatrix} \qquad (3a)$$

and its hermitean conjugate

$$S^{+}_{T}(f) = (\underline{S}^{*}_{1T}(f) \ldots \underline{S}^{*}_{nT}(f)) \qquad (3b)$$

in the following way:

$$C(f) = \lim_{T\to\infty} \frac{1}{2T} \langle S_T(f) \cdot S^{+}_{T}(f) \rangle. \qquad (4)$$

This is an abbreviated notation for

$$C(f) = \lim_{T\to\infty} \frac{1}{2T} \begin{bmatrix} \langle \underline{S}_{1T}(f)\,\underline{S}^{*}_{1T}(f) \rangle & \langle \underline{S}_{1T}(f)\,\underline{S}^{*}_{2T}(f) \rangle \ldots & \langle \underline{S}_{1T}(f)\,\underline{S}^{*}_{nT}(f) \rangle \\ \langle \underline{S}_{2T}(f)\,\underline{S}^{*}_{1T}(f) \rangle & \langle \underline{S}_{2T}(f)\,\underline{S}^{*}_{2T}(f) \rangle \ldots & \langle \underline{S}_{2T}(f)\,\underline{S}^{*}_{nT}(f) \rangle \\ \vdots & \vdots & \vdots \\ \langle \underline{S}_{nT}(f)\,\underline{S}^{*}_{1T}(f) \rangle & \langle \underline{S}_{nT}(f)\,\underline{S}^{*}_{2T}(f) \rangle \ldots & \langle \underline{S}_{nT}(f)\,\underline{S}^{*}_{nT}(f) \rangle \end{bmatrix} \qquad (5)$$

Formally, we can compute algebraic expressions using the complex amplitudes of windowed noise signals $\underline{S}_{iT}(f)$ in the same way as we would do it in the case of deterministic signals. $\underline{S}_{iT}(f)$ is the spectrum of a finite time segment of one concrete realization of the noise signal. It is possible in principle to record such a realization of a noise signal over a finite time interval. For this single case where we have measured the time dependence of the signal, we have the exact knowledge of the time dependence of the signal and may treat this signal as a deterministic signal. In our representation the change from the deterministic signal to the stochastic signal occurs when the averaging over the ensemble is performed. Without averaging, the correlation matrix, C(f), can be decomposed in the product of the signal vector $S_T(f)$ and its hermitean conjugate. In the case of deterministic signals, the ensemble averaging is of no influence since all elements of the ensemble are identical. The correlation matrix for deterministic signals has the rank one, and all signals are fully correlated. If we have statistical signals after the ensemble averaging process, it will be impossible to decompose the correlation matrix into a product of two vectors. For example, if we consider the n x n correlation matrix describing n statistically independent signal sources, the off diagonal elements of the correlation matrix will be zero. Statistically independent signals are represented by a diagonal correlation matrix.

For numerical computations with statistical signals, amplitude spectra of signals are not applicable. However, it is possible to compute the signal power spectra from the correlation spectra. There is a simple way to obtain the network equations for correlation spectra from the network equation for the amplitude spectra. Let $S_T(f)$ and $S'_T(f)$ be the vectors of a set of input and output signals of a linear network, and let M(f) be the coefficient matrix of the linear network equations. The network equations are given by

$$S'_T(f) = M(f) \cdot S_T(f). \qquad (6a)$$

The hermitean conjugate of the network equations is

$$S'^{+}_{T}(f) = S^{+}_{T}(f) \cdot M^{+}(f). \qquad (6b)$$

By multiplying Equation 6b from the left with Equation 6a, we obtain

$$S'_T(f) \cdot S'^{+}_{T}(f) = M(f) \cdot S_T(f) \cdot S^{+}_{T}(f) \cdot M^{+}(f). \qquad (7)$$

We now average over the ensemble and let $T\to\infty$, and using Equation 1 we obtain

$$C'(f) = M(f) \cdot C(f) \cdot M^{+}(f). \qquad (8)$$

If an n-port is represented by its admittance matrix, Y(f), the noise sources are described by equivalent current noise sources, $I^{Y}_{T}(f)$, in parallel to the n ports (Figure A).

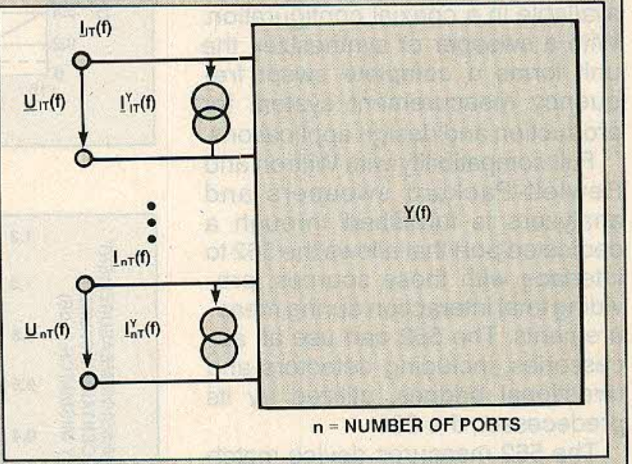

Fig. A Y-representation of a noisy n-port.

For the complex amplitude spectra we obtain

$$I_T(f) = Y(f) \cdot U_T(f) + I^{Y}_{T}(f), \qquad (9)$$

where the noise sources are described by

$$C^{Y}(f) = \lim_{T\to\infty} \frac{1}{2T} \langle I^{Y}_{T}(f) \cdot I^{Y+}_{T}(f) \rangle. \qquad (10)$$

References

1. R.A. Pucel, H.A. Haus and J. Statz, "Signal and Noise Properties of Gallium Arsenide Microwave Field-Effect Transistors," in *Advances in Electronics and Electron Physics*, New York, Academic Press, Vol. 38, 1975, pp. 195–265.
2. H. Fukui, "Optimal Noise Figure of Microwave GaAs MESFETs," IEEE Trans. Electron Devices, Vol. ED-26, July 1979, pp. 1032–1037.
3. H. Fukui, "Design of Microwave GaAs MESFET for Broadband Low Noise Amplifiers," IEEE Trans. on Microwave Theory and Techniques, Vol. MTT-27, July 1979, pp. 463–470.
4. H. Hillibrand and P.H. Russer, "An Efficient Method for Computer Aided Noise Analysis of Linear Amplifier Networks," IEEE Trans. on Circuits and Systems, April 1976, pp. 235–238.
5. A.M. Pavio, S.D. McCarter and P. Saunier, "A Monolithic Multistage 6-18 GHz Feedback Amplifier," IEEE Microwave and mm-Wave Monolithic Circuits Symposium Digest, June 1984, pp. 45–48.
6. T. McKay and R. Williams, "A High-Performance 2-18.5 GHz Distributed Amplifier: Theory and Experiment," IEEE MTT Symposium, June 1986.
7. Ulrich L. Rohde, "Designing a Matched Low Noise Amplifier Using CAD Tools," *Microwave Journal*, Oct. 1986, pp. 154–160.
8. Ulrich L. Rohde, "The Design of Wideband Amplifier with Large Dynamic Range and Low Noise Figure Using CAD Tools," 1987 IEEE Long Island MTT Symposium Digest, April 1987, pp. 47–55.
9. R.E. Lehmann and D.D. Heston, "X-Band Monolithic Series Feedback LNA," IEEE MTT Symposium, June 1985, pp. 55–59.